Master's Thesis of Science Education

Revised Estimation of Continental Water and Ice Mass Loss Pertinent to Sea Level Change

해수면 상승의 대륙별 기여도 재추정

February 2018

Graduate School of Science Education
Seoul National University
Earth Science Major

Jae-Seung Kim

Revised Estimation of Continental Water and Ice Mass Loss Pertinent to Sea Level Change

지도교수 서 기 원

이 논문을 교육학석사 학위논문으로 제출함

2017년 12월

서울대학교 대학원
과학교육과
김 재 승

김 재 승의 교육학석사 학위논문을 인준함
2018년 1월

위 원 장 이 준기 (인)
부위원장 서 기 원 (인)
위 원 이춘기 (인)

Abstract

Low degree spherical harmonics coefficients of Gravity Recovery and Climate Experiment (GRACE) gravity solutions contain large uncertainty due to its measurement limitation. In addition, residual PGR effect after its correction via numerical models remains in the GRACE gravity data and thus cause additional uncertainty in the estimate of regional and larger scale surface mass change. These inaccurate low degree coefficients in GRACE gravity data must be carefully considered when estimating water mass variations in regional scale. In this study, degree-1 and C_{21} and S_{21} coefficients in the association with surface mass distribution were estimated by the forward modeling incorporating self-attraction and loading effect to realize ocean mass changes. The PGR model error was mostly suppressed in the new estimates of degree-1 and C_{21} and S_{21} SH coefficients. Using the low degree SH coefficients, we re-evaluated ocean and continental mass variations. In particularly, we showed that terrestrial water mass depletion in Asia and North America is a significant contributor to the contemporary sea level rise.

Keyword : GRACE, Degree-1, C_{21}, S_{21}, Sea level, Mass budget

Student Number : 2016 - 21606

Contents

List of Figure

Chapter 1. Introduction

Global mean sea level (GMSL) rise is one of the most significant geophysical phenomena associated with global warming. Modern geodetical observational networks including tide gauges and satellite altimeters and gravimeter have successfully observed GMSL rise and helped to understand its cause. During 20th century, the rate of GMSL rise was about 1.44 mm/yr based on tide gauges measurement [*Church and White*, 2006], and its rate was found to be increased to 3.5 mm/yr from multiple satellite altimeters during the last decade [*Dieng et al.*, 2017]. The GMSL rise observed by tide gauges and satellite altimeters is caused by mainly two components; (1) ocean volume change resulting from ocean temperature and salinity variations and (2) ocean mass change due to water mass exchange among oceans, land and atmosphere. The volumetric effect can be observed by ARGO floats [*Leuliette and Miller*, 2009; *Willis et al.*, 2008], and ocean mass variations can be observed by Gravity Recovery and Climate Experiment (GRACE) satellite since May 2002 (e.g. *Chambers et al.* [2004]; *Chen et al.* [2005]). The ocean mass increase, 2.1 mm/yr , explains most of the GMSL rise [*Jeon et al.*, 2018].

The ocean mass change is closely affected by variations of ice sheet, glacier, and terrestrial water storage (TWS), and each contribution to GMSL rise also can be appraised by GRACE gravity data. Understanding their contribution to ocean mass is important to predict future sea level change and its global signature associated with self-attraction and loading (SAL) [*Farrell and Clark*, 1976]. The Greenland ice sheet (GrIS) mass loss was reported as -222 $\pm$ 9 Gt/yr during 2003-2010, which is equivalent to 0.6 mm/yr GMSL rise [*Jacob et al.*, 2012]. Melting of mountain glaciers was estimated as -196 Gt/yr [*Chen et al.*, 2013] albeit the signal is not clearly separable from TWS depletion due to sparse spatial resolution of GRACE. *Ramillien et al.* [2008] showed that the TWS decrease in large river basins has increased GMSL rise at a rate of 0.19 $\pm$ 0.06 mm/yr during 2003-2006. More recently, *Chen et al.* [2017] found the significant TWS decline in Caspian sea (-24.6 Gt/yr), and as a result GMSL increased about 0.06 mm/yr, implying that large scale TWS variation would play a non-negligible role in GMSL rise. The Antarctica also experienced large amount of ice mass loss, but its estimates based on GRACE were highly variable according to different studies. For example, *Chen et al.* [2013] estimated that Antarctic ice sheet (AIS) mass loss rate was about -180 Gt/yr (equivalent to 0.5mm/yr GMSL rise) during 2005–2011 while *Luthcke et al.* [2013] showed greatly reduced estimate, -80.8 Gt/yr (equivalent to 0.2mm/yr GMSL rise) during 2003–2010.

The divergent range of AIS mass loss rate is attributed to uncertainties in degrees 1 and 2 SH coefficients and imperfect correction of Post Glacial Rebound (PGR) in GRACE data. These limitations are also true for continental scale TWS variations. GRACE is not sensitive to the degree 1 SH coefficients, representing center of mass (CM) changes with respect to the center of figure (CF) of the Earth, and thus GRACE gravity solutions only include SH degree 2 and higher. According to *Wu et al.* [2012], the movement of CM by 1 mm/yr along the direction of the Earth rotation axis is equivalent to the effect of the 0.5 mm/yr of the GMSL and - 69

Gton/yr of the Antarctic ice mass loss. Therefore, the degree 1 coefficients need to be carefully considered for accurate examination of larger scale surface mass change. Furthermore, degree-2 terms (C_{20}, C_{21}, and S_{21}) of GRACE are generally replaced with other estimates (e.g., Satellite Laser Ranging (SLR), Earth Orientation Parameter (EOP)) due to their poor determination using GRACE platform [Chen et al. 2004, 2005]. The GRACE C_{20} coefficient has been reported to be vulnerable to alias effect, such as S_2 and K_2 tide [*Seo et al.*, 2008], and thus it has been commonly replaced by the C_{20} coefficient based on SLR [*Cheng et al.*, 2013]. C_{21} and S_{21} are also contaminated by the ocean pole tide [*Chen and Wilson*, 2008; *Wahr et al.*, 2015]], and *Wahr et al.* [2015] suggested methods to reduce its effect. PGR effect can be corrected using models (e.g., *A et al.* [2012]; *Ivins et al.* [2013]; *Paulson et al.* [2007]; *Peltier* [2004]; *Peltier et al.* [2015]), but its model-to-model difference in Antarctica is significant. *Barletta et al.* [2013] showed that modeled PGR effects equivalent to surface mass load in Antarctica ranged from 62.72 Gt/yr (*Ivins et al.* [2013]) to 140.65 (*Peltier* [2004]). Consequently, choice of a PGR model to correct its effect is particularly significant in AIS mass rate estimate.

Recently, *Jeon et al.* [2018] newly estimated degree 1 coefficients using forward modeling (FM) and SAL simulation, and also examined consistent check of reduced GRACE data by comparing observation of regional ocean mass with its prediction. The best agreement between observation and prediction was made when GRACE C_{20} after S_2 and K_2 aliasing correction, C_{21}/S_{21} based on EOP and ICE-6G PGR model (*Peltier et al.* [2015]) were used in GRACE data reduction. Based on the GRACE data reduction, they showed that rates of regional sea level rise vary significantly. However, the estimates of regional sea level variations are likely updated if a new PGR model is developed. In particular, uncertainty in C_{21}/S_{21} coefficients of PGR models is large due possibly to rotational feedback. Therefore, the recent estimates of regional ocean mass changes [*Jeon et al.*, 2018] and the continental water and ice mass contribution to sea level variations are likely affected by the PGR error.

In this study, we propose a new surface-mass-induced degree-1 and -2 SH coefficients by suppressing PGR model errors. These coefficients are used to re-estimate continental TWS and polar ice variations and ocean mass changes.

Chapter 2. Estimates of degree-1 and -2 coefficients

Previous studies examined low degree SH coefficients (e.g., degree 1 for geo-center motion and degree 2 for the dynamic oblateness of the Earth) by combining the terrestrial water and ice mass change observable from GRACE and the expected ocean mass variation [*Sun et al.*, 2016a; *Sun et al.*, 2016b; *Swenson et al.*, 2008]. *Swenson et al.* [2008] first suggested this method to estimate degree 1 SH coefficients, but the method did not include the realistic distribution of ocean mass associated with SAL effect and the correction for the contamination of land signal into oceans (leakage effect) caused by degree truncation. Later *Sun et al.* [2016a] modified the method by considering the SAL and leakage effects and estimated C_{20} coefficient together [*Sun et al.*, 2016b]. The leakage problem was reconciled by applying buffer zone between land and oceans. However, the modified method was limited in that optimum implementation parameters (e.g., degree truncation and buffer zone) were empirically selected via synthetic data. For example, they used fixed 200km butter zones for all monthly GRACE data and truncated SH coefficients up to degree and order 45 regardless of nature of time-varying signal strength over land.

In this study, we extend the previous method to estimate C_{21} and S_{21} as well as degree 1 SH coefficients simultaneously. Even though rotational feedback in C_{21} and S_{21} can be corrected [*Jeon et al.*, 2018; *Wahr et al.*, 2015], PGR error in both coefficients are large. Therefore, the coefficients should be newly examined for accurate estimates of the degree-1 SH coefficients and further large scale surface mass change. On the other hand, C_{20}, C_{22} and S_{22} are not estimated here because their PGR model-to-model differences are negligible. We also incorporate forward modeling (FM) (*Chen et al.* [2015]) to suppress leakage effect and apply SAL for a realistic sea level mass change. Here we briefly introduce the method [*Sun et al.*, 2016b; *Swenson et al.*, 2008], hereafter FM-SAL method, with some modification by inclusion of FM and SAL.

The SH coefficients we seek to estimate are summarized in $\bar{A}$:

$$\bar{\mathrm{A}} = \begin{bmatrix} C_{10} & C_{11} & S_{11} & C_{21} & S_{21} \end{bmatrix}^T \tag{1}$$

The same set of coefficients only for oceans, $\bar{A}_{ocean}$, can be estimated from SAL effect, which is derived by terrestrial water and ice mass redistribution from FM. Since we aim to estimate those five coefficients, FM is iterated without them. Initially, $\bar{A}$ can be estimated via the equation:

$$\bar{A}_{ocean} = \bar{I}\bar{A} + \bar{G} \tag{2}$$

The $\bar{I}$ and $\bar{G}$ are similar to those in *Swenson et al.* [2008] but extended to include C_{21} and S_{21} coefficients. For example,

$$\bar{I} = \frac{1}{4\pi} \int \bar{U}\bar{U}^T \, \vartheta(\theta\,, \phi) \; d\Omega \tag{3}$$

where $\bar{U}$ is given by

$$\bar{\mathrm{U}} = \begin{bmatrix} U_{C10} & U_{C11} & U_{S11} & U_{C21} & U_{S21} \end{bmatrix}^T \tag{4}$$

and the notation of $\bar{U}$ component is

$$U_{\psi lm} = \tilde{P}_{lm}(\cos\theta) \begin{cases} \cos(m\phi) \; (\psi = C) \\ \sin(m\phi) \; (\psi = S) \end{cases}, \tag{5}$$

in which θ and ϕ are colatitude and longitude, respectively; $\tilde{P}_{lm}$ is normalized associated Legendre functions; and $\vartheta(\theta\,,\phi)$ is the ocean function which is equal to zeros in land and ones in oceans. The $\bar{G}$ matrix consists of $\overline{U}$ and global SH coefficients estimated from FM for land and SAL for oceans:

$$G_{\psi lm} = \frac{1}{4\pi}\int U_{\psi lm}\,\vartheta(\theta,\phi)\sum_{l'=2}^{\infty}\sum_{m'=0}^{l'}\tilde{P}_{l'm'}(\cos\theta)\{C_{l'm'}\cos(m'\phi)+S_{l'm'}\sin(m'\phi)\}\,d\Omega \qquad (6)$$

Here the summations do not include degree (l') 2 and order (m') 1 terms since we aim to estimate the corresponding coefficients, C_{21} and S_{21}. Consequently, we can obtain the low degree global SH coefficients by repeatedly solving equation (2) with update of $\bar{A}_{ocean}$ until $\bar{A}$ converges.

Chapter 3. Synthetic experiment

3.1. Degree-1 and -2 SH coefficients

In order to verify the method above, we first synthesize GRACE-like data using various surface mass fields. The global land data assimilation system (GLDAS) [*Rodell et al.*, 2004] is adopted as terrestrial water balance except for glaciers and ice sheets, and the regional atmospheric climate model (RACMO2.3) [*Noël et al.*, 2015; *van Wessem et al.*, 2014] are as surface mass balance in Greenland Ice Sheet (GrIS) and Antarctic Ice Sheet (AIS). In addition, we combine ice mass loss rates in mountain glaciers and both ice sheets observed by GRACE [*Jacob et al.*, 2012] with the numerical model fields from GLDAS and RACMO2.3. Because the GRACE GSM data nominally do not include effects of barometric pressure and ocean dynamic, we do not consider them in the synthetic test. The ocean mass distribution is predicted by SAL simulation based on the composite of synthetic terrestrial surface mass field. A residual PGR signal is also taken into account by subtracting PGR models. We select three PGR models, which are proposed by *Paulson et al.* [2007] (PA), *A et al.* [2012] (AG), and *Peltier et al.* [2015] (PE) and consider three different PGR residuals, such as AG – PA (R_1), AG – PE (R_2), and PE – PA (R_3). Furthermore, we add GRACE error to the synthetic GRACE data. The error can be estimated by the difference between the GRACE GSM data and the smoothed GRACE GSM data, and the residual is decomposed by empirical orthogonal function analysis to finally select apparent noise that is random spatially and temporally [*Eom et al.*, 2017].

The black line of Figure 1(a) shows trend degree amplitudes of the synthetic surface mass fields including GRACE noise but excluding PGR error. Since GRACE cannot recover degree-1 coefficients, we remove them from the synthetic data. Red, blue and green lines of the same figure are estimated PGR errors of R_1(AG-PA), R_2(AG-PE), and R_3(PE-PA), respectively. The error from R_1 is smaller than others, and R_3 exhibits the largest error in degree-2. Therefore, combining the three PGR errors with surface mass field, we have three different synthetic GRACE data with different level of PGR errors. The larger errors in R_2 and R_3 are likely due to the different deglaciation history applied for the PGR models; PE model incorporates ICE-6G while AG and PA are based on ICE-5G. Likewise, because AG and PA models share the same ICE-5G deglaciation history, the error in R_1 is the smallest.

Figure 1(b) is the similar to Figure 1(a) after applying decorrelation filter and 500km Gaussian smoothing for the synthetic data and PGR errors. Figure 1(a) clearly exhibits that PGR errors are apparent at degree-2, and after spatial filtering (Figure 1(b)), the degree-2 PGR error is more dominant relative to higher degree PGR errors. However, at degree 3 and higher SH coefficients, amplitudes of smoothed synthetic GRACE data shown in Figure 1(b) are much larger than those of PGR errors. Consequently, degrees-1 and -2 SH coefficients estimated by the FM-SAL method using SH coefficients higher than degree 2 would include mostly water and ice mass variations with minor influence of PGR errors.

To examine the PGR error in degree-2 SH coefficients in detail, time variations of synthetic degree-2 SH coefficients are shown in Figure 2. Black lines are ‘true’ coefficients, and red, blue, and green lines are contaminated coefficients

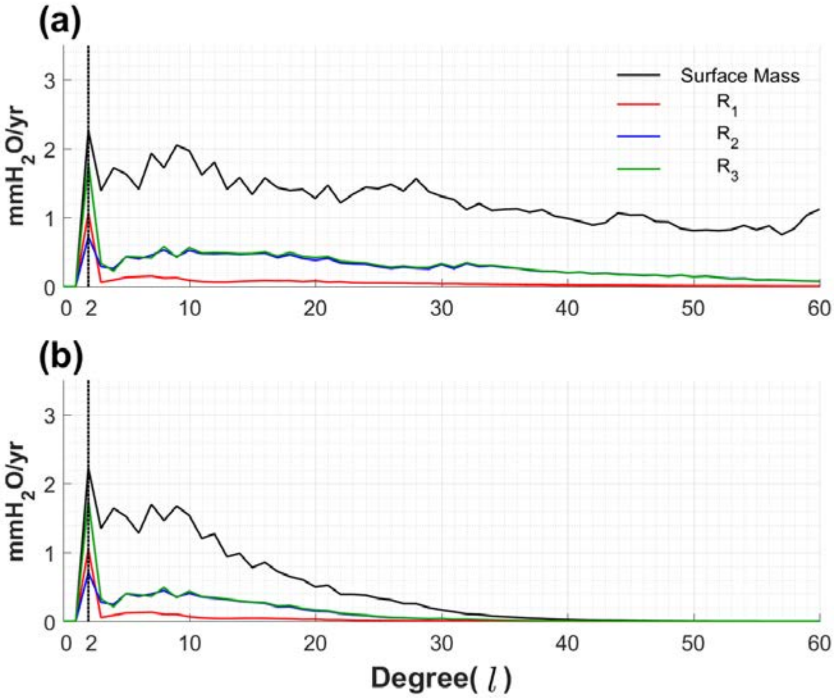

Figure 1. (a) Trend degree amplitudes in synthetic GRACE data (black), and PGR errors of R_1 (red), R_2 (blue) and R_3 (green) cases. (b) Similar to (a) except for applying spatial filtering (decorrelation filter and Gaussian smoothing).

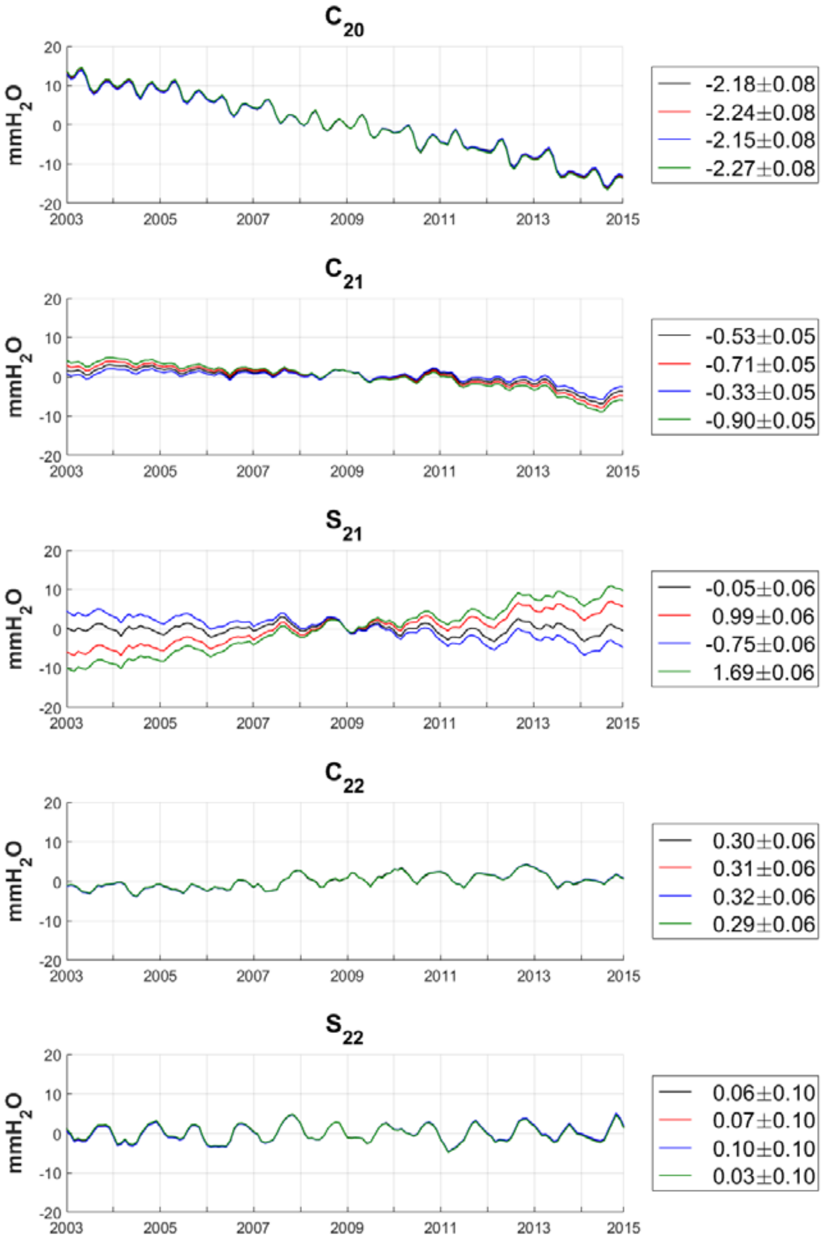

Figure 2. Time series of degree-2 SH coefficients contaminated by PGR errors of R_1 (red), R_2 (blue) and R_3 (green). Black solid lines represent time series of the true coefficients. Linear trends (mmH_2O/yr) with 95% confidence interval are shown.

from PGR errors of AG – PA (R_1), AG – PE (R_2), and PE – PA (R_3), respectively. The PGR model discrepancies in C_{20}, C_{22} and S_{22} SH coefficients are negligible, and the apparent errors are evident in C_{21} and S_{21} SH coefficients. This result indicates that recovery of large scale surface mass change from GRACE would be problematic due to the C_{21} and S_{21} uncertainty associated with PGR error as well as the missing degree-1 SHs. Therefore, as discussed above, in this study, we aim to estimate degree-1 SH coefficients that GRACE cannot recover and C_{21} and S_{21} SH coefficients that are largely contaminated by PGR errors.

After removing the degree-1 and -2 SH coefficients from the synthetic data, we estimate them using the FM-SAL method. Since PGR error in C_{20}, C_{22} and S_{22} SH coefficients are negligible, we do not estimate them using the FM-SAL method. Figure 3 shows the estimated degree-1 coefficients. Black lines show 'true' synthetic degree-1 coefficients associated with surface mass load, and red, blue and green lines are recovered degree-1 SH coefficients when the synthetic GRACE data are contaminated by PGR errors of AG – PA (R_1), AG – PE (R_2), and PE – PA (R_3), respectively. Regardless of PGR errors, the recovered coefficients are very close to the true ones except C_{10} with R_2 and R_3 cases. As shown in Figures 1 and 2, the PGR model errors of R_2 and R_3 are larger than that of R_1, and which indicates that larger PGR errors in higher SH degree leak into the C_{10} estimate. As discussed above, the larger error is associated with the different deglaciation history.

Figure 4 shows estimated C_{21} and S_{21} SH coefficients from the synthetic data. Similar to previous figures, black lines are 'true' synthetic SH coefficients associated with water and ice mass redistribution. Red, blue, and green lines are estimated ones by the FM-SAL method using SH coefficients higher than degree-2 that are contaminated by PGR model errors of R_1, R_2 and R_3, respectively. The estimated time-series closely agree with the true ones, indicating that the PGR errors in both coefficients shown in Figure 2 are significantly reduced.

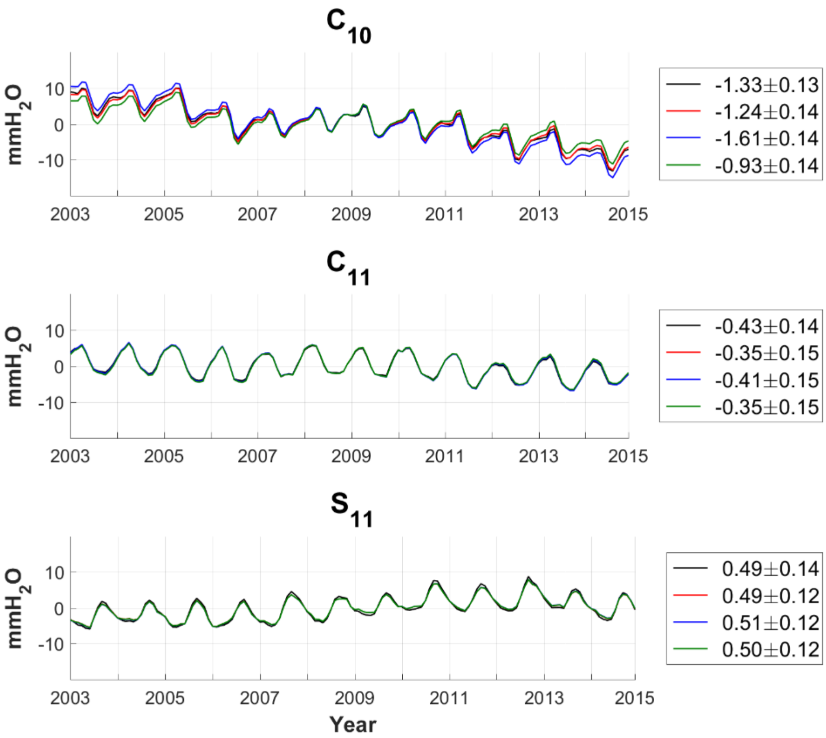

Figure 3. Time series of recovered C_{10} (top), C_{11} (middle), and S_{11} (bottom) using synthetic data contaminated by PGR residuals of R_1 (red), R_2 (blue) and R_3 (green). Black solid lines represent time series of the true coefficients. Linear trends (mmH_2O/yr) with 95% confidence interval are shown.

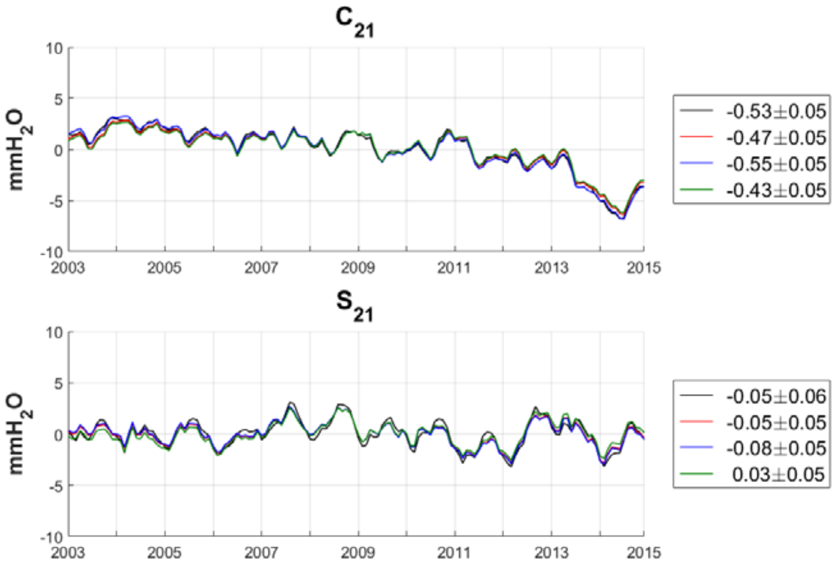

Figure 4. Time series of recovered C21 and S11 using synthetic data contaminated by PGR residuals of R1 (red), R2 (blue) and R3 (green). Black solid lines represent time series of the true coefficients. Linear trends (mmH2O/yr) with 95% confidence interval are shown.

3.2. Oceanic and continental mass change

Using the estimated degree-1 and C_{21} and S_{21} SH coefficients, we examine oceanic and continental mass variations. Figure 5 shows the true ocean mass variations (black lines) and the estimated ones (red, blue and green lines for R_1, R_2 and R_3 cases, respectively) by including the degree-1 and C_{21} and S_{21} SH coefficients shown in Figures 3 and 4. Linear trends within 95% confidence interval are shown in each panel. Estimated oceanic variations (red, blue and green lines) closely agree with the true variations (black lines) even though the synthetic data were contaminated by different PGR model errors. However, there is relatively poor agreement in the Arctic Sea due to the C_{10} uncertainties shown in Figure 3 particularly for the green line recovered from the R_3 PGR error. Similarly, Figure 6 represents the true and the recovered time-series of the water mass changes in all continents. In most continents, the true and the recovered solutions show good agreement with one another. However, in Asia, North America, and Antarctica, the continental mass loss rates vary significantly even though the PGR error in C_{21} and S_{21} SH coefficients are mostly diminished. This result indicates that recovery of continental surface mass load is largely affected by PGR errors at SH degree-3 and higher coefficients, which cannot be corrected in the FM-SAL method.

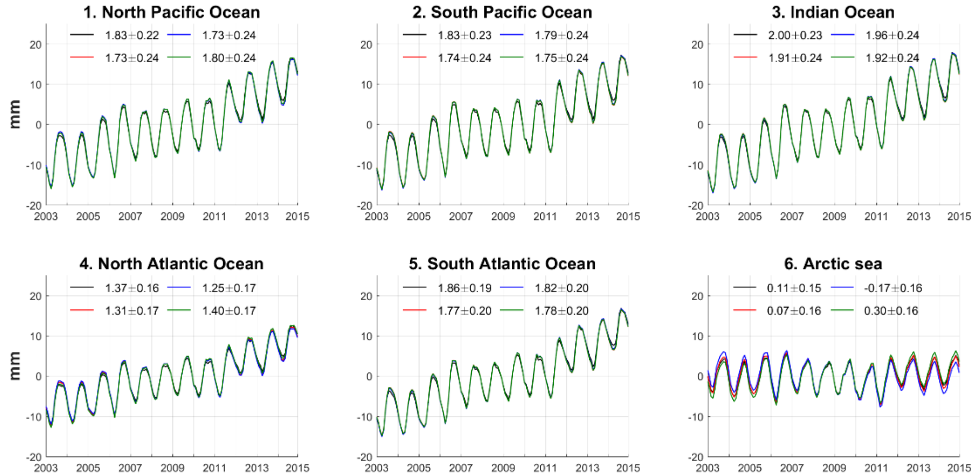

Figure 5. True (black) and recovered ocean mass variations (red, blue and green).

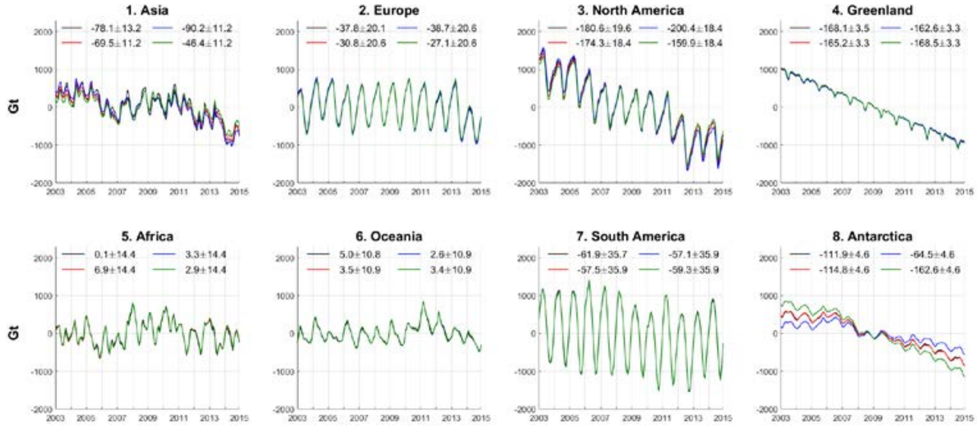

Figure 6. True (black) and recovered continental mass variations (red, blue and green).

Chapter 4. Degree-1 and -2 coefficients from GRACE

In this section, we estimate the surface-mass-induced degree-1 and degree-2 SH coefficients based on GRACE gravity solutions (CSR, release 5) for the period from 2003 to 2014. The PGR effect in the GRACE observation is removed by the three models used in the synthetic experiment, and thus there are three post-processed GRACE data with different level of un-modeled PGR error. Similar to the synthetic case, we apply decorrelation filter and 500km Gaussian smoothing to suppress spatially correlated aliasing error and random noise, respectively. Figure 7 shows the degree-2 SH coefficients from real GRACE data after PGR effect was reduced by AG (red), PA (blue) and PE (green) models. Similar to the synthetic case shown in Figure 2, the PGR-corrected C_{21} and S_{21} coefficients do not agree with one another implying that larger uncertainty in PGR models for the coefficients. As implied in Figure 2, PGR error in C_{20}, C_{22} and S_{22} coefficients is apparently negligible, and thus we do not consider them here.

As in the synthetic experiment, we first estimate the degree-1 SH coefficients using FM-SAL method (Figure 8). Similar to the synthetic experiment shown in Figure 3, regardless of PGR corrections, trends of C_{11} and S_{11} are very close to one another. However, C_{10} trends show relatively large discrepancy while the differences are not as large as those shown in Figure 3. This result indicates that un-modeled PGR effect in real GRACE data is likely less significant than the synthetic cases. Our estimates are compared with the previous studies (Table 1). Trends in our

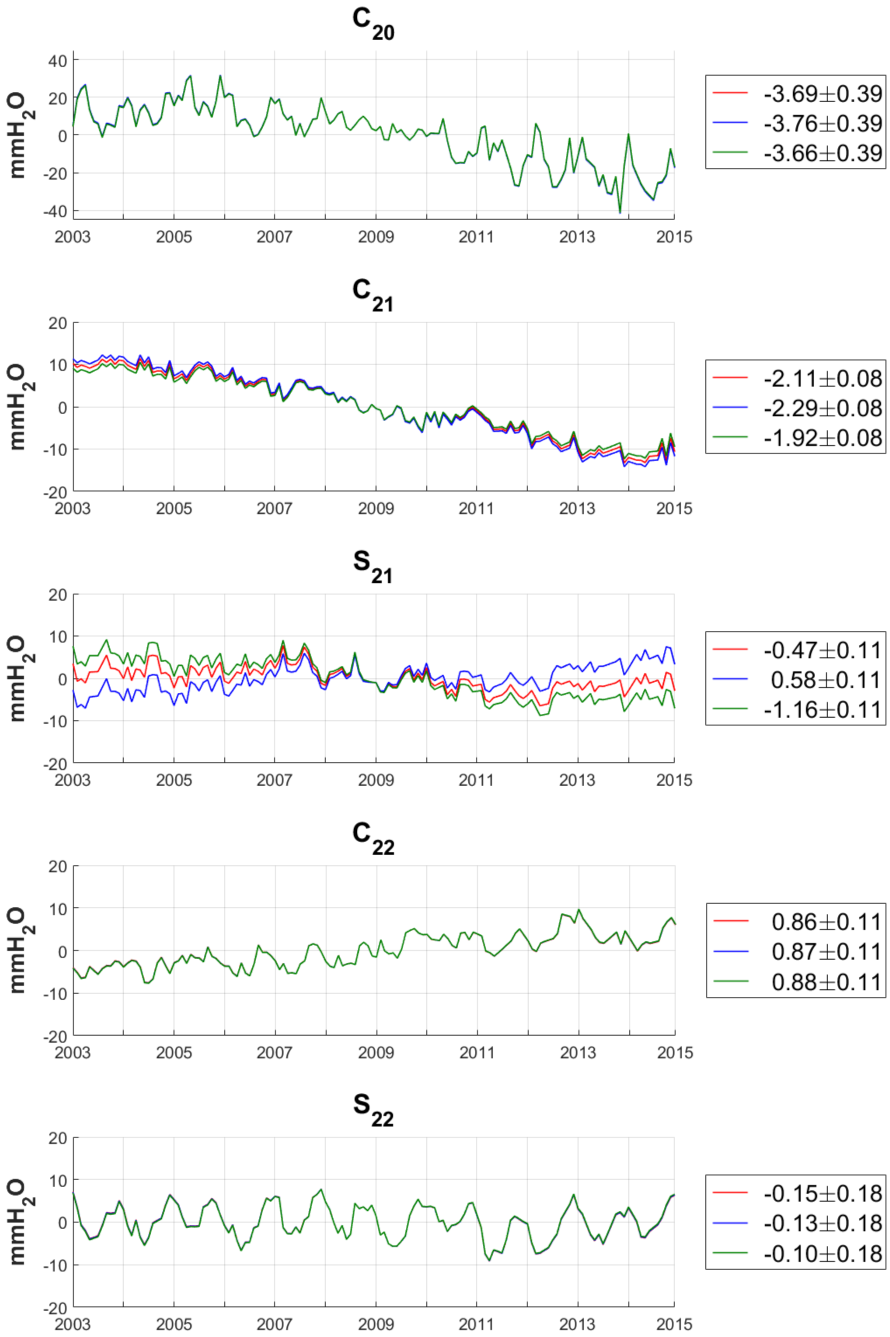

Figure 7. Time series of degree-2 SH coefficients contaminated by PGR models of AG (red), PA (blue) and PE (green).

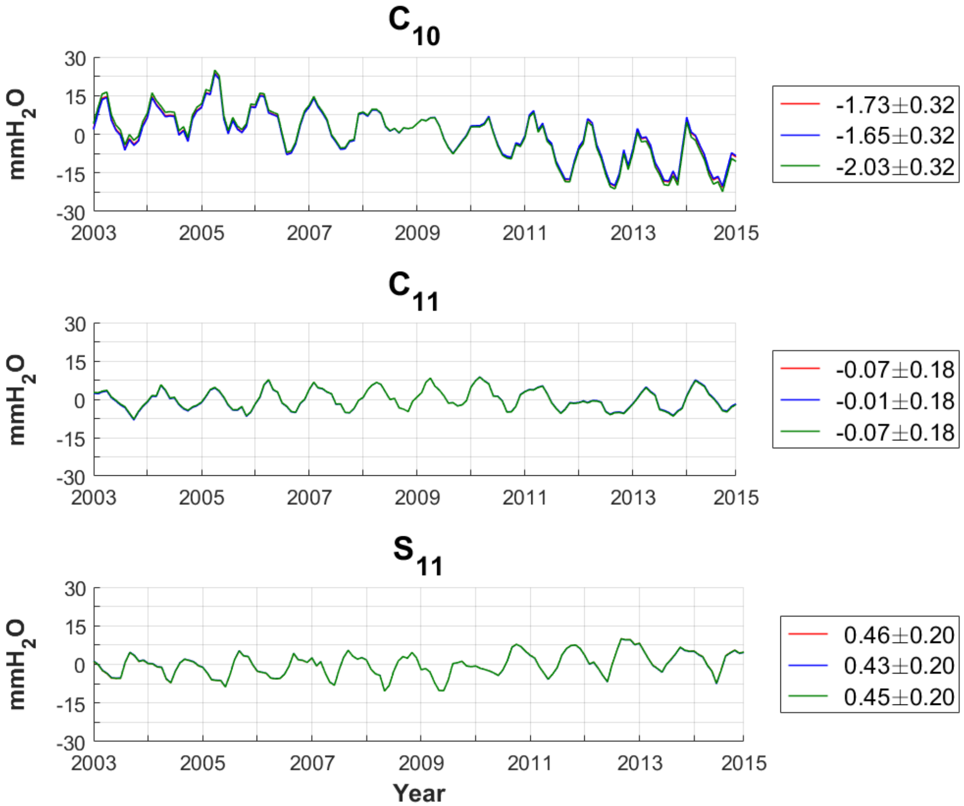

Figure 8. Time series of recovered C_{10} (top), C_{11} (middle), and S_{11} (bottom) using GRACE data corrected by PGR models: AG (red), PA (blue) and PE model (green).

Table 1. Trends of degree-1 coefficients suggested by previous studies and this study.

		C_{10} (mmH_2O/yr)	C_{11} (mmH_2O/yr)	S_{11} (mmH_2O/yr)
Swenson et al. [2008]		-0.78 ± 0.21	-0.31 ± 0.15	-0.04 ± 0.18
Sun et al. [2016b]		-1.14 ± 0.31	-0.17 ± 0.19	0.39 ± 0.20
Jeon et al. [2018]		-2.31 ± 0.30	-0.25 ± 0.18	-0.02 ± 0.20
This study	AG correction	-1.73 ± 0.32	-0.07 ± 0.18	0.46 ± 0.20
	PA correction	-1.65 ± 0.32	-0.01 ± 0.18	0.43 ± 0.20
	PE correction	-2.03 ± 0.32	-0.07 ± 0.18	0.45 ± 0.20

estimates are larger than the results of *Swenson et al.* [2008] and *Sun et al.* [2016b]. As discussed above, our method differs from the previous studies; *Swenson et al.* [2008] did not consider SAL effect and the both studies empirically corrected leakage effects. Even though *Jeon et al.* [2018] used the same FM-SAL method with PGR correction of PE, the previous trends in the dgree-1 coefficients differ from here. The differences are caused by the PGR error in C_{21} and S_{21} SH coefficients in the previous study. As shown in Figure 7, PGR errors are large in both coefficients, and the errors leak into other SH coefficients during forward modeling and SAL simulation in the previous study. However, in this study, we estimate them with the degree-1 SH coefficients simultaneously, and thus nominally the estimated degree-1 SH coefficients are not contaminated by the PGR error in C_{21} and S_{21}. Figure 9 shows the estimates of C_{21} and S_{21} using the FM-SAL method. Large PGR error shown in Figure 7 are significantly reduced and the three estimates agree with each other within 95% confidence level.

To examine PGR error reduction in C_{21} and S_{21} SH coefficients, we compare SAL simulation and GRACE observation over oceans. If the PGR effect, which is particularly large in C_{21} and S_{21} SH coefficients, was effectively reduced by a model, the reduced GRACE SH coefficients mostly represent surface mass load with relatively minor residual of PGR effect. If so, observed GRACE ocean mass ought to be the same as the simulated ocean mass using the FM-SAL method [*Jeon et al.*, 2018]. Figure 10a shows the trend difference between GRACE observation and FM-SAL simulation over oceans [*Jeon et al.*, 2018]. PE model was used to remove PGR effect and GRACE C_{20} after correcting S_2 and K_2 aliasing error was incorporated.

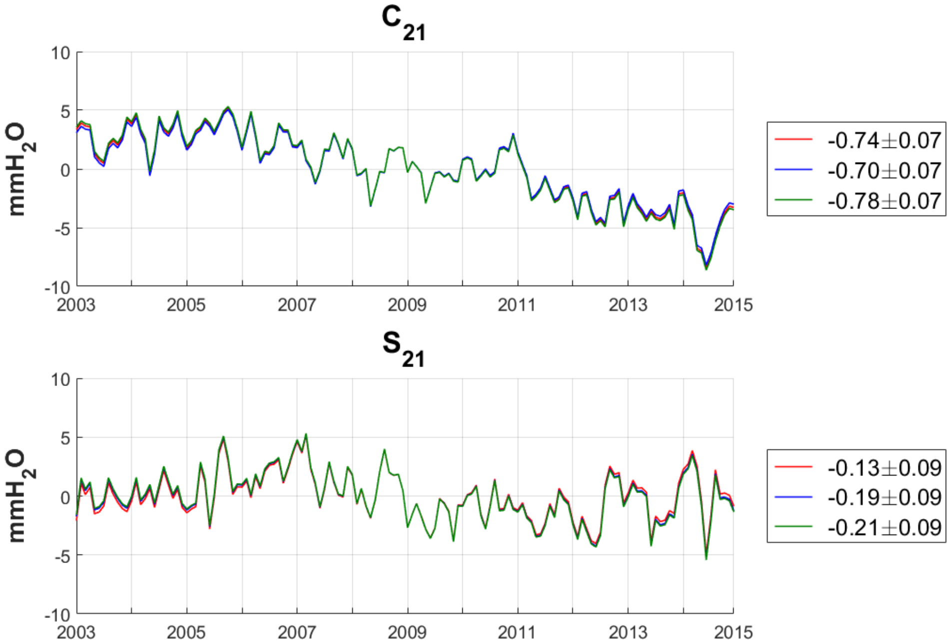

Figure 9. Time series of recovered C_{21} and S_{11} using GSM data corrected by PGR models: AG (red), PA (blue) and PE (green).

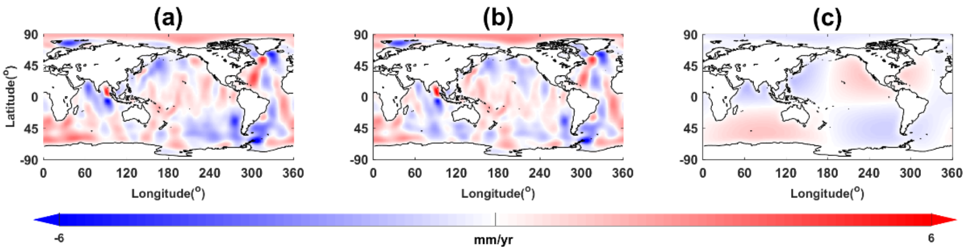

Figure 10. Trend difference maps between GSM observation and SAL prediction. (a) is the result of *Jeon et al.* [2018]. (b) is the result when PGR error in C_{21} and S_{21} of *Jeon et al.* [2018] is corrected by the FM-SAM method. (c) represents the difference between (a) and (b) panel. The unit of data is mm per year.

Effects that cannot be simulated by the FM-SAL but can be observable from GRACE are clearly exhibited; there are gravity signal associated with GRACE error and residual ocean dynamics, which is un-modeled ocean bottom pressure in GRACE de-aliasing process [*Quinn and Ponte*, 2011], and post seismic deformations [*Han et al.*, 2006]. Furthermore, the trend map shows a large scale anomaly pattern associated with degree 2 and order 1 SH coefficients, which is likely the PGR error in C_{21} and S_{21} coefficients. Figure 10(b) is the similar to the Figure 10(a) except replacing GRACE C_{21} and S_{21} SH coefficients with those estimated from the FM-SAL method. Figure 10(c) is the difference between Figures 10(a) and 10(b) and clearly exhibits the degree 2 and order 1 anomaly. This result indicates again that large scale PGR error in C_{21} and S_{21} SH coefficients is effectively suppressed by the FM-SAL method.

Chapter 5. Oceanic and continental mass change from GRACE

With improved estimates of degree-1 and C_{21} and S_{21} SH coefficients, we re-evaluate sea level change associated with ocean mass variations and continental water mass change. Figure 11 shows the regional sea level changes associated with the PGR correction of AG (red), PA (blue) and PE (green) models. Yellow lines exhibit the similar ocean mass change from the conventionally post-processed GRACE data recommended by GRACE Tellus (https://grace.jpl.nasa.gov/), which includes degree-1 of *Swenson et al.* [2008], C_{20} from SLR [*Cheng et al.*, 2013], C_{21} and S_{21} of *Wahr et al.* [2015] and AG PGR model. Leakage effects from terrestrial surface mass change are corrected using the FM-SAL method [*Jeon et al.*, 2018], and seasonal variations are removed. Our new estimates show close agreement regardless of PGR model selection. This is because the large PGR error in C_{21} and S_{21} is corrected by the FM-SAL method. On the other hand, our estimates differ significantly from those based on the conventional GRACE post-processing. Numbers in italic font at each panel represent linear trends from the similar FM-SAL method incorporating PE model but did not considering PGR model errors [*Jeon et al.*, 2018]. The previous estimates [*Jeon et al.*, 2018] contaminated by PGR error in C_{21} and S_{21} are larger than new estimates particularly for the North Atlantic Ocean.

Similar to Figure 11, Figure 12 shows the continental water mass changes after seasonal cycles are corrected. The three estimates after PGR corrections in C_{21} and

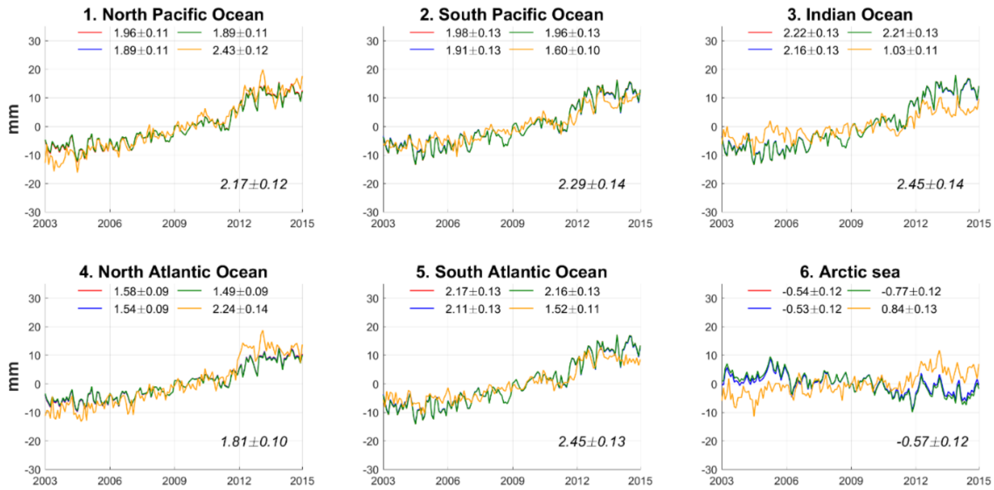

Figure 11. Ocean mass variations from GRACE data corrected by new estimates of degree-1 and C_{21} and S_{21} SH coefficients. The PGR effect is suppressed by the PGR models of AG (red), PA (blue) and PE (green). Seasonal cycles are removed. Yellow lines are the similar ocean mass changes from GRACE data that is reduced by the commonly recommended post-process: degree-1 of *Swenson et al.* [2008]; C_{20} of SLR [*Cheng et al.*, 2013]; C_{21} and S_{21} of *Wahr et al.* [2015]; AG model [*A et al.*, 2012]. The italic number in each panel represents the trend based on *Jeon et al.* [2018].

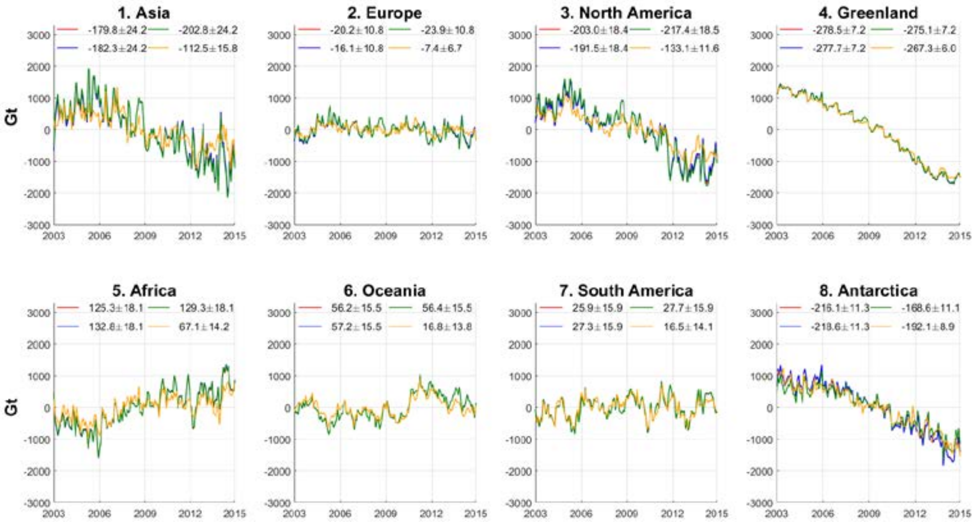

Figure 12. Continental mass variations from GRACE data corrected by new estimates of degree-1 and C_{21} and S_{21} SH coefficients. The PGR effect is suppressed by the PGR models of AG (red), PA (blue) and PE (green). Seasonal cycles are removed. Yellow lines are the similar continental mass changes from GRACE data that is reduced by the commonly recommended post-process: degree-1 of *Swenson et al.* [2008]; C_{20} of SLR [*Cheng et al.*, 2013]; C_{21} and S_{21} of *Wahr et al.* [2015]; AG model [*A et al.*, 2012]. The italic number in each panel represents the trend based on *Jeon et al.* [2018].

S_{21} coefficients agree with one other within 95% confidence interval except for Antarctica; the green line (PGR correction with PE) exhibits much lower ice mass loss rate than others. New estimates also show that continental TWS changes significantly contribute the present-day sea level variations. TWS decrease in Asia and North America are larger or about equivalent to the ice mass loss in Antarctica. Mass loss associated with mountain glacier melting in both continents partly explain the TWS decrease; *Jacob et al.* [2012] estimated that glacier mass loss in Asia and North America during 2003-2010 were -7 Gt/yr and -108 Gt/yr, respectively. However, this result indicates that soil moisture and groundwater depletion also play major roles in the contemporary sea level rises. On the other hand, TWS increase in Africa mitigates sea level rise.

Chapter 6. Conclusion

We estimated the degree-1 and C_{21}, and S_{21} SH coefficients whose PGR error was suppressed by the FM-SAL method, and the linear trends of each coefficient were within 95% confidence interval regardless of the PGR model selection. In particular, GRACE data corrected by the new estimates of C_{21} and S_{21} coefficients showed better consistency between the GRACE observation and the SAL prediction than the previous result of *Jeon et al.* [2018]. With those surface-mass-induced coefficients, we re-estimated regional sea level and continental water mass changes. Due to effective reduction of PGR errors in C_{21} and S_{21}, the regional water mass variations in oceans as well as continents showed close agreement regardless of PGR model choice except in Antarctica. PGR error reduction in C_{21} and S_{21} SH coefficients revealed the significant contribution of TWS depletion to the present-day sea level rise particularly in Asia and North America.

Reference

A, G., J. Wahr, and S. Zhong (2012), Computations of the viscoelastic response of a 3-D compressible Earth to surface loading: an application to Glacial Isostatic Adjustment in Antarctica and Canada, *Geophysical Journal International*, *192*(2), 557-572, doi:10.1093/gji/ggs030.

Barletta, V. R., L. S. Sørensen, and R. Forsberg (2013), Scatter of mass changes estimates at basin scale for Greenland and Antarctica, *The Cryosphere*, *7*(5), 1411-1432, doi:10.5194/tc-7-1411-2013.

Chambers, D. P., J. Wahr, and R. S. Nerem (2004), Preliminary observations of global ocean mass variations with GRACE, *Geophysical Research Letters*, *31*(13), n/a-n/a, doi:10.1029/2004gl020461.

Chen, J. L., and C. R. Wilson (2008), Low degree gravity changes from GRACE, Earth rotation, geophysical models, and satellite laser ranging, *Journal of Geophysical Research*, *113*(B6), doi:10.1029/2007jb005397.

Chen, J. L., C. R. Wilson, J. Li, and Z. Z. Zhang (2015), Reducing leakage error in GRACE-observed long-term ice mass change: a case study in West Antarctica, *Journal of Geodesy*, *89*(9), 925-940, doi:10.1007/s00190-015-0824-2.

Chen, J. L., C. R. Wilson, and B. D. Tapley (2013), Contribution of ice sheet and mountain glacier melt to recent sea level rise, *Nature Geoscience*, *6*(7), 549-552, doi:10.1038/ngeo1829.

Chen, J. L., C. R. Wilson, B. D. Tapley, J. S. Famiglietti, and M. Rodell (2005), Seasonal global mean sea level change from satellite altimeter, GRACE, and geophysical models, *Journal of Geodesy*, *79*(9), 532-539, doi:10.1007/s00190-005-0005-9.

Chen, J. L., C. R. Wilson, B. D. Tapley, H. Save, and J.-F. Cretaux (2017), Long-term and seasonal Caspian Sea level change from satellite gravity and altimeter measurements, *Journal of Geophysical Research: Solid Earth*, doi:10.1002/2016jb013595.

Cheng, M., B. D. Tapley, and J. C. Ries (2013), Deceleration in the Earth's oblateness, *Journal of Geophysical Research: Solid Earth*, *118*(2), 740-747, doi:10.1002/jgrb.50058.

Church, J. A., and N. J. White (2006), A 20th century acceleration in global sea-level rise, *Geophysical Research Letters*, *33*(1), n/a-n/a, doi:10.1029/2005gl024826.

Dieng, H. B., A. Cazenave, B. Meyssignac, and M. Ablain (2017), New estimate of the current rate of sea level rise from a sea level budget approach, *Geophysical Research Letters*, *44*(8), 3744-3751, doi:10.1002/2017gl073308.

Eom, J., K.-W. Seo, and D. Ryu (2017), Estimation of Amazon River discharge based on EOF analysis of GRACE gravity data, *Remote Sensing of Environment*, *191*, 55-66, doi:10.1016/j.rse.2017.01.011.

Farrell, W. E., and J. A. Clark (1976), On Postglacial Sea Level, *Geophysical Journal of the Royal Astronomical Society*, *46*(3), 647-667, doi:10.1111/j.1365-246X.1976.tb01252.x.

Han, S. C., C. K. Shum, M. Bevis, C. Ji, and C. Y. Kuo (2006), Crustal dilatation observed by GRACE after the 2004 Sumatra-Andaman earthquake, *Science*, *313*(5787), 658-662, doi:10.1126/science.1128661.

Ivins, E. R., T. S. James, J. Wahr, E. J. O. Schrama, F. W. Landerer, and K. M. Simon

(2013), Antarctic contribution to sea level rise observed by GRACE with improved GIA correction, *Journal of Geophysical Research: Solid Earth*, *118*(6), 3126-3141, doi:10.1002/jgrb.50208.

Jacob, T., J. Wahr, W. T. Pfeffer, and S. Swenson (2012), Recent contributions of glaciers and ice caps to sea level rise, *Nature*, *482*(7386), 514-518, doi:10.1038/nature10847.

Jeon, T., K.-W. Seo, K. Youm, J. Chen, and C. R. Wilson (2018), Global sea level change signatures observed by GRACE satellite gravimetry.

Leuliette, E. W., and L. Miller (2009), Closing the sea level rise budget with altimetry, Argo, and GRACE, *Geophysical Research Letters*, *36*(4), doi:10.1029/2008gl036010.

Luthcke, S. B., T. J. Sabaka, B. D. Loomis, A. A. Arendt, J. J. McCarthy, and J. Camp (2013), Antarctica, Greenland and Gulf of Alaska land-ice evolution from an iterated GRACE global mascon solution, *Journal of Glaciology*, *59*(216), 613-631, doi:10.3189/2013JoG12J147.

Noël, B., W. J. van de Berg, E. van Meijgaard, P. Kuipers Munneke, R. S. W. van de Wal, and M. R. van den Broeke (2015), Summer snowfall on the Greenland Ice Sheet: a study with the updated regional climate model RACMO2.3, *The Cryosphere Discussions*, *9*(1), 1177-1208, doi:10.5194/tcd-9-1177-2015.

Paulson, A., S. Zhong, and J. Wahr (2007), Inference of mantle viscosity from GRACE and relative sea level data, *Geophysical Journal International*, *171*(2), 497-508, doi:10.1111/j.1365-246X.2007.03556.x.

Peltier, W. R. (2004), GLOBAL GLACIAL ISOSTASY AND THE SURFACE OF THE ICE-AGE EARTH: The ICE-5G (VM2) Model and GRACE, *Annual Review* *of Earth and Planetary Sciences*, *32*(1), 111-149, doi:10.1146/annurev.earth.32.082503.144359.

Peltier, W. R., D. F. Argus, and R. Drummond (2015), Space geodesy constrains ice age terminal deglaciation: The global ICE-6G_C (VM5a) model, *Journal of Geophysical Research: Solid Earth*, *120*(1), 450-487, doi:10.1002/2014jb011176.

Quinn, K. J., and R. M. Ponte (2011), Estimating high frequency ocean bottom pressure variability, *Geophysical Research Letters*, *38*(8), n/a-n/a, doi:10.1029/2010gl046537.

Ramillien, G., S. Bouhours, A. Lombard, A. Cazenave, F. Flechtner, and R. Schmidt (2008), Land water storage contribution to sea level from GRACE geoid data over 2003–2006, *Global and Planetary Change*, *60*(3-4), 381-392, doi:10.1016/j.gloplacha.2007.04.002.

Rodell, M., et al. (2004), The Global Land Data Assimilation System, *Bulletin of the American Meteorological Society*, *85*(3), 381-394, doi:10.1175/BAMS-85-3-381.

Seo, K.-W., C. R. Wilson, J. Chen, and D. E. Waliser (2008), GRACE's spatial aliasing error, *Geophysical Journal International*, *172*(1), 41-48, doi:10.1111/j.1365-246X.2007.03611.x.

Sun, Y., P. Ditmar, and R. Riva (2016a), Observed changes in the Earth's dynamic oblateness from GRACE data and geophysical models, *J Geod*, *90*, 81-89, doi:10.1007/s00190-015-0852-y.

Sun, Y., R. Riva, and P. Ditmar (2016b), Optimizing estimates of annual variations and trends in geocenter motion and J2 from a combination of GRACE data and geophysical models, *Journal of Geophysical Research: Solid Earth*, *121*(11), 8352-8370, doi:10.1002/2016jb013073.

Swenson, S., D. Chambers, and J. Wahr (2008), Estimating geocenter variations from a combination of GRACE and ocean model output, *J Geophys Res-Sol Ea*, *113*(B8), B08410, doi:10.1029/2007jb005338.

van Wessem, J. M., C. H. Reijmer, J. T. M. Lenaerts, W. J. van de Berg, M. R. van den Broeke, and E. van Meijgaard (2014), Updated cloud physics in a regional atmospheric climate model improves the modelled surface energy balance of Antarctica, *The Cryosphere*, *8*(1), 125-135, doi:10.5194/tc-8-125-2014.

Wahr, J., R. S. Nerem, and S. V. Bettadpur (2015), The pole tide and its effect on GRACE time-variable gravity measurements: Implications for estimates of surface mass variations, *Journal of Geophysical Research: Solid Earth*, *120*(6), 4597-4615, doi:10.1002/2015jb011986.

Willis, J. K., D. P. Chambers, and R. S. Nerem (2008), Assessing the globally averaged sea level budget on seasonal to interannual timescales, *Journal of Geophysical Research*, *113*(C6), doi:10.1029/2007jc004517.

Wu, X., J. Ray, and T. van Dam (2012), Geocenter motion and its geodetic and geophysical implications, *Journal of Geodynamics*, *58*, 44-61, doi:10.1016/j.jog.2012.01.007.

국문초록

해수면 상승의 대륙별 기여도 재추정

서울대학교 대학원
과학교육과 지구과학 전공
김 재 승

Gravity Recovery and Climate Experiment (GRACE) 중력 해의 저차 구면 조화함수 계수는 중력위성의 관측 한계로 인해 큰 불확실성을 포함하고 있다. 또한 GRACE 자료를 이용하여 종관규모의 지표 질량 변동을 연구할 때, Post-glacial rebound (PGR) 보정 후 남아 있는 잔여 효과는 추가적인 불확실성을 야기한다. 그러므로 광역적인 물 질량 변동을 연구할 때 GRACE 중력해의 저차항들은 주의 깊게 다루어져야 한다. 본 연구에서는 순산 모델링 (forward modeling) 기법과 실제 바다 질량 변화를 구현하기 위한 self-attraction and loading 효과를 함께 이용하여 지표질량이 만들어내는 degree-1, C_{21} 및 S_{21} 계수를 추정하였다. 새롭게 추정된 degree-1, C_{21} 및 S_{21} 계수에는 PGR 보정 후 남아있는 오차가 대부분 감쇄되었으며, 이 계수들은 해양 및 대륙의 물질량 변동을 재추정하는데 적용되였다. 그 결과 북미와

아시아의 육수 질량의 고갈은 현재 해수면 상승에 크게 기여하고 있음이 확인되었다.

주요어 : GRACE, Degree-1, C21, S21, 해수면 변화, 육지 수질량 변화
학번 : 2016 - 21606